Geomechanics and Engineering, *Vol. 9, No. 3 (2015) 373-395*
DOI: http://dx.doi.org/10.12989/gae.2015.9.3.373

Improvement of pavement foundation response with multi-layers of geocell reinforcement: Cyclic plate load test

Omid Khalaj [*1], Seyed Naser Moghaddas Tafreshi [2a],
Bohuslav Mašek [1b] and Andrew R. Dawson [3c]

[1] *The Research Centre of Forming Technology, University of West Bohemia, Plzen, Czech Republic*
[2] *Department of Civil Engineering, K.N. Toosi University of Technology, Tehran, Iran*
[3] *Nottingham Transportation Engineering Centre, University of Nottingham, Nottingham, UK*

(*Received January 26, 2015, Revised April 30, 2015, Accepted May 10, 2015*)

Abstract. Comprehensive results from cyclic plate loading at a diameter of 300 mm supported by layers of geocell are presented. The plate load tests were performed in a test pit measuring 2000 × 2000 mm in plane and 700 mm in depth. To simulate half and full traffic loadings, fifteen loading and unloading cycles were applied to the loading plate with amplitudes of 400 and 800 kPa. The optimum embedded depth of the first layer of geocell beneath the loading plate and the optimum vertical spacing of geocell layers, based on plate settlement, are both approximately 0.2 times loading plate diameter. The results show that installation of the geocell layers in the foundation bed, increase the resilient behavior in addition to reduction of accumulated plastic and total settlement of pavement system. Efficiency of geocell reinforcement was decreased by increasing the number of the geocell layers for all applied stress levels and number of cycles of applied loading. The results of the testing reveal the ability of the multiple layers of geocell reinforcement to 'shakedown' to a fully resilient behavior after a period of plastic settlement except when there is little or no reinforcement and the applied cyclic pressure are large. When shakedown response is observed, then both the accumulated plastic settlement prior to a steady-state response being obtained and the resilient settlements thereafter are reduced. The use of four layers of geocell respectively decreases the total and residual plastic settlements about 53% and 63% and increases the resilient settlement 145% compared with the unreinforced case. The inclusion of the geocell layers also reduces the vertical stress transferred down through the pavement by distributing the load over a wider area. For example, at the end of the load cycle of the applied pressure of 800 kPa, the transferred pressure at the depth of 510 mm is reduced about 21.4%, 43.9%, 56.1% for the reinforced bases with one, two, and three layers of geocell, respectively, compared to the stress in the unreinforced bed.

Keywords: cyclic loading; multiple geocell layers; pavement foundation; residual and resilient deformations

---

*Corresponding author, Post-Doctoral Research Fellow, E-mail: khalaj@vctt.zcu.cz
[a] Professor, E-mail: nas_moghaddas@kntu.ac.ir
[b] Professor, E-mail: masekb@kmm.zcu.cz
[c] Associate Professor, E-mail: andrew.dawson@nottingham.ac.uk

http://www.techno-press.org/?journal=gae&subpage=7 ISSN: 2005-307X (Print), 2092-6219 (Online)

1. Introduction

In the last decades, use of geosynthetic (planar and cellular) reinforced soil has made significant impact in geotechnical engineering applications e.g., road construction layers, railway embankments, pavement system, uplift behavior of anchors, footing, slope and earth stabilization and lifeline provision (e.g., Collin *et al*. 1996, Raymond 2002, Yoon *et al*. 2004, Ghosh *et al*. 2005, Patra *et al*. 2005, Hufenus *et al*. 2006, Dash *et al*. 2007, Madhavi Latha and Rajagopal 2007, El Sawwaf 2007, Bathurst *et al*. 2009, Zhang *et al*. 2010, Pokharel *et al*. 2010, Madhavi Latha 2011, Boushehrian *et al*. 2011, Koerner 2012, Yang *et al*. 2012, Tavakoli Mehrjardi *et al*. 2012, Leshchinsky and Ling 2013, Niroumand and Anuar Kassim 2013, Tanyu *et al*. 2013, Sireesh *et al*. 2013, Chen *et al*. 2013, Tandel *et al*. 2014, Deb and Konai 2014, Keskin 2015). Recent studies have been shown that geocell reinforcement can be significantly more effective than a planar reinforcement, in improving the behaviour of foundation beds under static and repeated loads (Moghaddas Tafreshi and Dawson 2010a, b). The three dimensional geometry of geocell i.e., the superior confinement offered by the geocells in all directions, allows the soil in the cells to develop a passive resistance that increases the soil's bearing capacity and decreases the settlement of the foundation bed.

Sireesh *et al*. (2009) carried out a series of laboratory scale model tests on a circular footing supported by reinforced soil with single layer of geocell overlying clay bed with a continuous circular void. They reported that substantial improvement in performance can be obtained with the provision of geocell mattress, of adequate size, over the clay subgrade with void and beneficial effect could be obtained when the geocell mattress spread beyond the void at least a distance equal to the diameter of the void. Thakur *et al*. (2012) investigated the performance of single geocell-reinforced recycled asphalt pavement (RAP) bases, reporting that the geocell-reinforced RAP bases had much smaller permanent deformations and smaller vertical stresses than unreinforced base.

Geosynthetic inclusions would be most effective if used in the zone significantly stressed by the loading surface (e.g., footing or tire wheel) – which may be over a depth of 1 or 2 width/diameters beneath the footing/tire wheel – i.e., over a depth of approximately 0.6 – 2 m for typical footing widths and over a depth of 0.3 – 0.6 m for typical tire wheel widths. Since, the heights of commercially produced geocells are usually standard and manufacturers of geocell produce them at heights less than 200 mm (available cell depths produced by two key manufacturers in Europe and the USA), using a 0.6 to 2 m single thick layer of geocell beneath the footing and tire wheel is not possible for field construction. Even if it were, such a thick geocell layer would likely make compaction of cell-fill extremely difficult (Thakur *et al*. 2012), consequently decreasing the performance of a thick single layer of geocell. Hence, the use of several layers of geocell (say, three or four) each with a thickness ≤ 200 mm and with vertical spacing between successive layers of geocell is a practical alternative and could be a beneficial means of reinforcing the soil beneath a loading surface. Although it might be anticipated that more geocell layers in a foundation bed reduce the deformations, but there is much detail of the use of multiple geocell layers under repeatedly applied loads which would have application, potentially, to pavement foundation (or machine support) systems.

Hence, in the current research, the overall goal was to demonstrate the benefits of introducing multi-layered geocell reinforcement to address weak spots in pavement foundations (e.g., at trench reinstatements). Cyclic loading conditions were selected as these are of particular concern for pavement (or machine foundation) problems where localized soil reinforcement might be appropriate. Thus a total of 19 independent cyclic plate load tests (plus 10 repeated tests) of a pavement foundation supported on unreinforced soil or soil reinforced with geocell were performed in a test pit measuring 2000 × 2000 mm in plane and 700 mm in depth using a 300 mm diameter rigid steel plate. Testing was arranged so as to determine the parameters controlling best usage. The various parameters studied in this testing program include the optimal depth of the top geocell layer, the optimal vertical spacing between successive layers of geocell, the effects of the number of geocell layers on settlements of loading surface and the effects of the geocell layers on the stress profile with depth of foundation bed.

2. Test materials

2.1 Soil

Granular soil passing through the 38 mm sieve with a specific gravity of 2.68 (G_s = 2.68) was used as backfill soil in the testing program. It was sourced from a local quarry and satisfies the criteria and limitations recommended in ASTM D 2940-09. The grading of this soil is presented in Fig. 1(a) (ASTM D422-07). According to the Unified Soil Classification System (ASTM D 2487-11), the sand is classified as well graded sand with letter symbol *SW*. According to the modified proctor compaction tests (ASTM D 1557-12), the maximum dry density was about 20.62 kN/m^3, which corresponds to an optimum moisture content of 5.7% (see Fig. 1(b)). The angle of internal friction (φ) of sand obtained through triaxial tests at a wet density of 19.58 kN/m^3 (corresponding to 90% of maximum dry density) was 40.5°. This soil was used to fill the geocell and to place between the geocell layers.

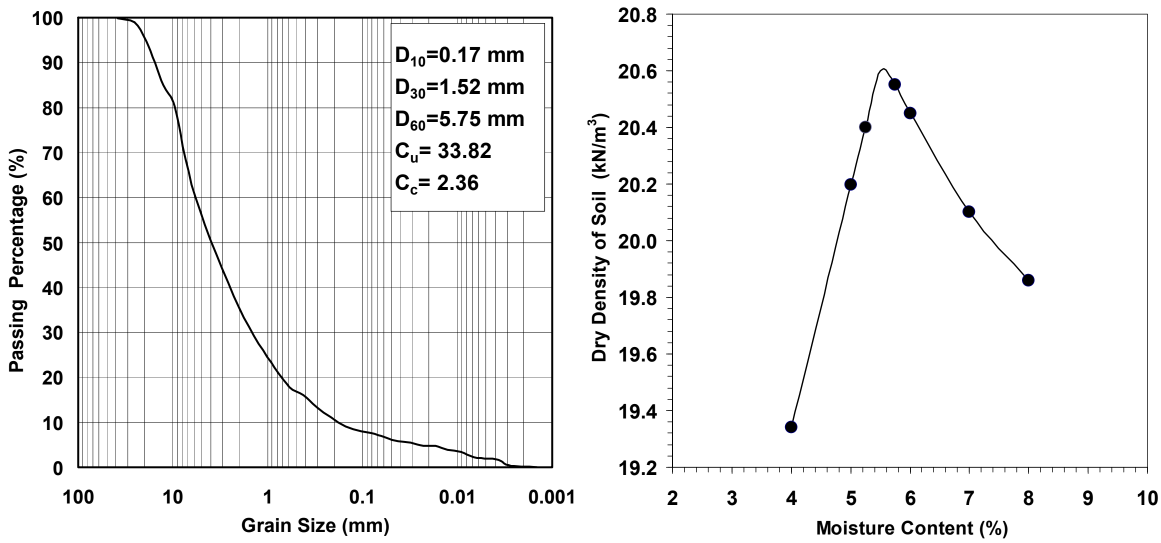

(a) Grain size distribution curve (b) compacted curve

Fig. 1 Grain size distribution curve and compacted curve for backfill soil

2.2 Geocell

The geocell used in the current study was fabricated from, non-woven geotextile, comprising continuous polypropylene filaments, thermo-welded to form an imperforated "honeycomb" arrangement (Fig. 2). This type of geocell reinforcement, when filled with soil or other mineral material, provides confinement chambers due to the frictional and passive resistance developed at the soil-geocell interfaces. It prevents the lateral displacement of infill, thus increasing the bearing pressure and hindering the subsidence of foundation beds. To achieve the maximum performance of geocell reinforcement (i.e., full mobilization of the frictional and passive resistance at the soil-geocell interfaces), the geocell pockets must be expanded at its maximum sizes in width and length.

According to the manufacturer, the strength and stiffness of the geocell joint is higher or similar to that of the geocell wall material (i.e., geotextile). The engineering properties of the geotextile from which geocell is formed and the geometry of the geocell, as listed by the manufacturer, are

Fig. 2 A close view of expanded geocell spread in the test pit

Table 1 The engineering properties of the geotextile used in the tests

Description	Value
Type of geotextile	Non-woven
Material	Polypropylene
Mass per unit area (gr/m^2)	190
Thickness under 2 kN/m^2 (mm)	0.57
Thickness under 200 kN/m^2 (mm)	0.47
Tensile strength (kN/m)	13.1
Strength at 5% (kN/m)	5.7
Effective opening size (mm)	0.08
Height of cells, h_g (mm)	100
Geocell pocket size (Width and length of cells), d (mm)	110

presented in Table 1. Maximum Geocell pocket size (d = 110 mm) and height of geocell (h_g = 100 mm) were kept constant. The ratio of the maximum geocell pocket size (d = 110 mm) to diameter of loading plate (D = 300 mm) is, thus, 0.37 (d/D = 0.37). Dash *et al.* (2001) in their studies on strip footings supported by geocell-reinforced sand reported that the bearing capacity of footing increases with decrease in pocket size, due to the overall increase in confinement effect of geocell pockets and rigidity of the mattress. As the pocket size increases, the confinement reduces and hence the soil freely moves out of the pockets leading to smaller load carring capacity. They recommended d/D ratio less than 0.8 times of footing width to ignore local effects and to deliver good performance improvement. Rajagopal *et al.* (1999) have also observed similar influence of the pocket size on the behaviour of geocell-reinforced sands. It should be noted that for the small footing diameter relative to the size of the geocell, local effects might be created by the position of the cell walls relative to the footing. However, the d/D ratio adopted may not the optimum value and a change in d/D might change the results. The effect of d/D could be investigated in future studies.

3. Experimental program

3.1 Model test setup

The stress on RSC corresponding to 40 mm of settlement is found to be 70% greater than that of OSC diameTo investigate the performance improvement in the deformation and the stress profile of pavements supported by layers of geocell, a full scale model test of a standard plate load was conducted in an outdoor test pit. The test pit, measuring 2000 mm × 2000 mm in plan, and 700 mm in depth, was excavated in natural ground to construct the geocell layers and to install the pressure cells. The schematic cross-section of the test set-up of the foundation bed containing geocell layers, the loading plate model, loading system and data measurement system (dial gauges and soil pressure cells), the geometry of the test configurations, and location of three soil pressure cells, is shown in Fig. 3.

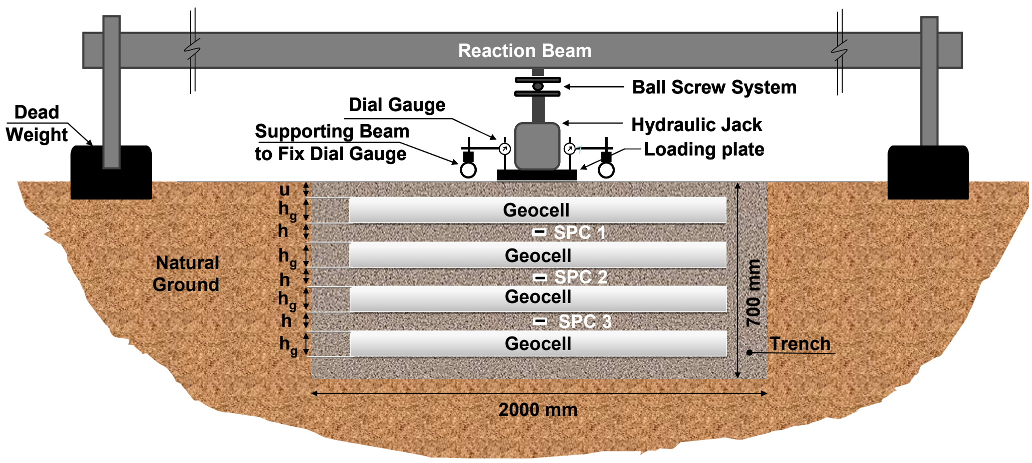

Fig. 3 Schematic cross-section of the test set-up (not to scale), “SPC 1”, “SPC 2”, and “SPC 3” indicate the location of three soil pressure cells

A hand operated hydraulic jack imposed by a manually-operated pump and supported against a strong reaction frame applied loads on a steel rigid circular plate (as a loading surface) of 300 mm diameter and 25 mm in thickness located on the centre of the trench surface. An additional 10 mm thick rubber base was attached at the bottom of the loading plate to simulate the rubber tire contact with the ground surface. Although, the distributed pressure by a tire wheel passage might be rather different from the distributed pressure by rigid plate load with an additional 10 mm thick rubber base, but it can deliver useful results in the absence of flexible tire wheel load test (Kim and Tutumluer 2005, ASTM D 1195-09 2009). However, this limitation in the present work isn't expected to be very influential on the outcomes and the effect of flexible tire wheel could be also investigated in future studies. Also, the hydraulic jack applied loading on the pre-calibrated load cell with a capacity of 4000 kg and an accuracy of ± 0.01% full scale which was located between the loading shaft and circular plate (soil surface) and connected to a load cell reader.

To measure the vertical stress inside the foundation bed, it was instrumented with three full bridged, 50 mm diameter diaphragm-type soil pressure cells (SPC). These had an accuracy of 0.1% of full range of 1000 kPa according to the manufacturer. The top soil pressure cell (abbreviated to "SPC 1"), middle soil pressure cell ("SPC 2"), and bottom soil pressure cell ("SPC 3") are located at 190 mm, 350 mm, and 510 mm beneath the center of loading plate (Fig. 3). The instruments were connected to digital converters and the output data was recorded in mV and then converted to real stress units using established calibrations for the sensors. To ensure an accurate reading, three pressure cells were calibrated prior to each test series. Since the pressure cells are located at the middle of soil layers (see Fig. 3, the soil layers between to geocell layers), to simulate the real test condition and to obtain the calibrations for the pressure cells, a 300 mm-diameter and 200 mm-high cylinder container made of very soft textile was filled with the backfill soil and each cell was placed, in turn, in the middle. Thereafter, by placing the container with the pressure cell in the middle, in a compression machine, the pressure cells were calibrated for different levels of cyclic applied pressure. Also, to measure the movement of the plate, throughout the tests, three linear dial gauges with an accuracy of 0.01% of full range (100 mm) were attached to a reference beam and their tips placed about 10 mm inwards from the edge of the plate. Also, a photograph of the test installation prior to testing, showing the reaction beam, load plate, hydraulic jack and three dial gauges is presented as Fig. 4.

Fig. 4 Photograph of test installation prior to loading include reaction beam, load plate, hydraulic jack and three dial gauges

3.2 Compaction of backfill layers

In order to compact the layers of the foundation including unreinforced soil and geocell-reinforced layers, a walk-behind vibrating plate compactor, 450 mm in width, was used. In all the tests, the compactor passed over the backfill at ten levels being 0, 60, 160, 220, 320, 380, 480, 540, 640, and 700 mm from the level of the base of the loading plate. To achieve the required density of backfill layers, in all tests, the soil layers and the soil that filled the geocell pockets were compacted at an optimum moisture content of 5.7% with two and three passes, respectively so that the compactive effort, and consequently compaction energy, was kept the same for all passes of the compactor. To better assess the layers' compaction, three sand cone tests in accordance with ASTM D 1557-12 (2012) were conducted in some installations and after layer compaction, to measure the densities and moisture content of compacted soil layers and the density of the soil filled into the geocell pockets. The density values measured in the three cone tests revealed a close match with maximum differences in results of only a rather small 1-1.5%. The average measured (recovered) moisture content of the layers was between 5.2% and 5.7%. To prevent loss of moisture from the backfill during the load test, the exposed backfill was covered to a distance of 1.8 m from the circumference of the bearing plate with a waterproof paper. The average measured dry densities (average of three sand cone tests) of unreinforced soil and the soil filled in geocell pockets after compaction of each layers were about 18.52 kN/m^3 (approximately 90% of maximum soil dry density) and 18 kN/m^3 (approximately 87% of maximum soil dry density), respectively.

3.3 Loading pattern

The loading arrangements were chosen to represent the tires of typical trucks on a pavement. While general traffic loading will not be applied to the geocell-aggregate layers but millions of times to overlying asphalt layers, such loading will be applied for a few traffic passages during construction and this will, likely, be the most demanding time for the reinforced foundation. In addition, AASHTO T 221-90 (2010) and ASTM D 1195-09 (2009) recommend application a few load cycles using repetitive static plate load tests of flexible pavement for use in evaluation and design of airport and highway pavements. It is this loading which was simulated in the work described here by distributing wheel loads over an equivalent circular area at the appropriate tire pressure (Brito *et al*. 2009).

Hence, in order to simulate the effect of wheel loading, unloading and reloading were imposed through the plate at a rate of 1.5 kPa per second. The maximum applied pressure of 800 kPa was chosen to replicate that of a heavy vehicle half-axle with "Super-Single" tire, as used on a common heavy trailer (6 axles and a mean pressure 792 kPa) (Brito *et al*. 2009). In Test Series 1 and 4 (see Table 2), the maximum applied pressure of 800 kPa was divided into two stages being 400 and 800 kPa to simulate half and full traffic loadings. For each stage, fifteen loading and unloading cycles were applied as shown in Fig. 5. Preliminary repeated load tests (which are not reported in the paper) showed that (regardless of the number of geocell layers), with increase in the number of load cycles, the rate of change of loaded surface settlements reduces, so that their response has become, approximately, stable within fifteen load cycles at the low level of cyclic pressure (400 kPa). The interest was to establish the likelihood of such a response being disturbed by a greater cyclic pressure (800 kPa). Overall, this implies that a large number of cyclic load applications were not essential. Also, in order to save time in Test Series 2 and 3 (see Table 2), only one load cycle for each of the six cyclic pressures (150, 300, 400, 600 kPa) was applied on the loading plate.

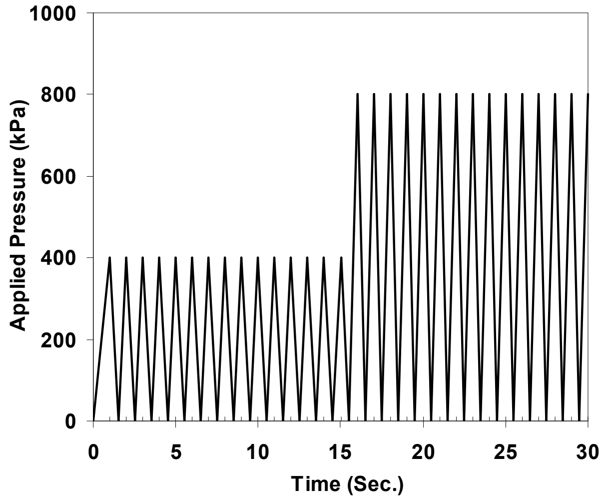

Fig. 5 Pattern of repeated load on loading plate

4. Test parameters and testing program

The geometry of the test configurations for the multi-layered geocell is shown in Fig. 3. In addition, Table 2 gives details of all the test series done in this study. Test Series 1 provided reference, unreinforced, performance data. In the case of the geocell reinforced bed, three series of tests (Test Series 2, 3 and 4) were conducted by varying the depth of the first layer of geocell reinforcement beneath the loading surface (u), the vertical spacing of the geocell layers (h), and the number of geocell layers (N).

The width of the geocell layers (b) and the depth to the top of the first geocell layer below the loading surface (u) are expressed in non-dimensional form with respect to loading plate diameter

Table 2 Scheme of the cyclic plate load tests for unreinforced pavement and multi-layered geocell-reinforced pavement

Test series	Type of test	N	u/D	h/D	No. of tests	Purpose of the tests
1	Unreinforced	--------	-------		1+2*	To quantify the improvements due to reinforcements
**2	Geocell reinforced	1	0, 0.1, 0.13, 0.17, 0.2, 0.25, 0.3, 0.6, 1	-------	9+4*	To arrive at the optimum values of u/D and h/D
**3		2	0.2	0.15, 0.2, 0.25, 0.4, 0.8	5+2*	
4		1, 2, 3, 4	0.2	0.2	4+2*	To investigate the effect of the number of geocell layers

*The tests which were performed two or three times to verify the repeatability of the test data
**In order to save time, only one load cycle of 150, 300, 400, 600 kPa pressure were applied

(D = 300 mm) as, b/D and u/D. In line with the findings of Moghaddas Tafreshi and Dawson (2012), Dash *et al*. (2003), Yoon *et al*. (2008) and Thakur *et al*. (2012), the parameter b/D was held constant in all the tests at b/D = 5. The variable parameter, h, is used to describe the vertical spacing between the bottom of the previous layer of geocell and the top of the next layer. It is expressed in non-dimensional form with respect to loading plate diameter (D) as h/D, whereas the height of geocell layers (h_g) is expressed in dimensional form equal to 100 mm.

Note that, for the unreinforced installation (Test Series 1) and the geocell reinforced installation with one layer of geocell (Test Series 4), the top, middle, and bottom soil pressure cells ("SPC 1", "SPC 2", and "SPC 3") are installed. In order to prevent damage to the soil pressure cells, for the reinforced bases with two layers of geocell (Test Series 4), only the middle and bottom soil pressure cells ("SPC 2" and "SPC 3"), and for the reinforced bases with three layers of geocell (Test Series 4), only the bottom soil pressure cells ("SPC 3") are installed. For the reinforced bases with four layers of geocell (Test Series 4) and for the Test Series 2 and 3, no pressure cells are installed.

In order to assess the utility of the apparatus, the accuracy of the measurements, the repeatability of the system, the reliability of the results and finally to verify the consistency of the test data, many of the tests described in Table 2 were repeated at least twice. The results obtained revealed a close match between results of the two or three trial tests with maximum differences in results of around 6-8%. This difference was considered to be small and is subsequently neglected. The consistency of the results demonstrates that the procedure and technique adopted can produce repeatable tests within the bounds that may be expected from geotechnical testing apparatus. It should be noted that after each plate load test, including the repeat tests, all the backfill from the test pit was removed and installed again by the explained procedure in Section 3.2.

5. Results and discussions

The performance improvement due to the provision of geocell reinforcement in the plate settlement and the distributed pressure at depth of the pavement foundation beds is represented here using two non-dimensional improvement factors:

(1) Improvement in the loading surface settlement (*PRS*: Percentage Reduction Settlement) which compares the total (peak) and residual plastic settlements of the geocell reinforcement bed to that of the unreinforced bed at the same applied cyclic pressure and the same load cycle. *PRS* uses for total settlement (abbreviated to "PRS_{total}") and for residual plastic settlement (abbreviated to "$PRS_{resid.}$").
(2) Improvement in the loading surface settlement (*PES*: Percentage Enhancement Settlement) which compares the resilient settlement of the geocell reinforcement bed to that of the unreinforced bed at the same applied cyclic pressure and the same load cycle.
(3) Improvement in the distributed pressure at depth of the pavement foundation bed (*PRP*: Percentage Reduction Pressure) which compares the distributed pressure at depth of the geocell reinforcement bed to that of the unreinforced bed at the same applied cyclic pressure and the same load cycle. They are defined as follows

$$PRS = \left(1 - \frac{s_{geocell}}{s_{unrein.}}\right) * 100 \tag{1}$$

$$PES_{resil.} = \left(\frac{s_{geocell}}{s_{unrein.}} - 1 \right) * 100 \tag{2}$$

$$PRP = \left(1 - \frac{q_{geocell}}{q_{unrein.}} \right) * 100 \tag{3}$$

Where s_{unrein} and $s_{geocell}$ are the values of plate settlement (it could be the total, residual plastic or resilient settlements) of the unreinforced bed and the geocell reinforced bed at the same applied cyclic pressure and the same load cycle, respectively. Also q_{unrein} and $q_{geocell}$ are the values of the distributed pressure at depth of the geocell reinforcement bed to that of the unreinforced bed at the same applied cyclic pressure and the same load cycle, respectively.

5.1 The optimum value of u/D ratio

The optimum value of the u/D ratio is obtained from Test Series 2 in Table 2. The tests are done for different depths of placement of a single layer of geocell reinforcement ($N = 1$), below the loading plate (u/D). In these tests, only one load cycle was applied at the surface of loading plate. Fig. 6 shows the variation of the percentage reduction in total settlement (PRS_{total}) and in residual plastic settlement ($PRS_{resid.}$) with u/B ratio at different amplitudes of cyclic load (= 150, 300, 400, 600 kPa). From this figure, it is found that the percentage reduction in total and residual settlements (PRS_{total} and $PRS_{resid.}$) initially increasing when u/B increases from zero, up to approximately u/D = 0.2-0.25, but that, thereafter, the value of PRS_{total} and PRS_{res} decrease with depth of placement, irrespectively of amplitude of cyclic load. The increase in performance improvement until $u/D \approx$ 0.2-0.25 could be due to the surface soil layer, above the geocell reinforcement, acting as a cushion, preventing the direct contact of the loading plate base with the cell walls and distributing the footing pressure more uniformly over the cellular geocell. The other probable reason that these u/D values are optimal is that at smaller cover thicknesses, the soil mass above the geocell reinforcing layer provides insufficient overburden to generate the required friction resistance at the interface between the geocell layer and the soil. Insufficient confining pressure on the top geocell layer beyond the footing edges is also possible at low depth ratio values. The similar findings for footings has been reported by Sitharam and Sireesh (2005), Yoon *et al*. (2008) and Moghaddas Tafreshi and Dawson (2010a, 2012). As the value of u/D increases beyond 0.2-0.25 (toward 1), the top geocell layer moves to be out of the zone where it can most successfully interrupt the applied stress field and, hence, the PRS_{total} and PRS_{res} values decrease (i.e. total and plastic settlements increase). Finally, as expected, with increase in u/D ratio to about one, the geocell layer lies almost entirely outside of the significantly stressed zone under the loading plate, the influence of reinforcement thus becomes negligible, and the overall response approaches that of an unreinforced pavement foundation. For example, from Fig. 6(b) at 600 kPa amplitude of applied load, the PRS_{res} values are about 41%, 46%, 67%, 61%, 19%, and 3% for u/D equal to 0, 0.1, 0.2, 0.3, 0.6, and 1, respectively. This example shows that the maximum reduction in plastic settlement (i.e. the minimum value of plastic settlement) occurs at a u/D value of approximately 0.2.

Although the optimum u/D value might be a function of loading plate size, the height of geocell layers, the geocell pocket size, type of soil and the number of geocell layers, in the present study,

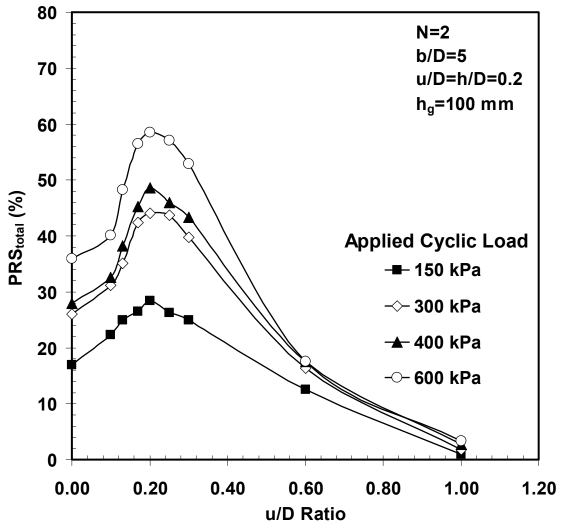

(a) PRS_{total}

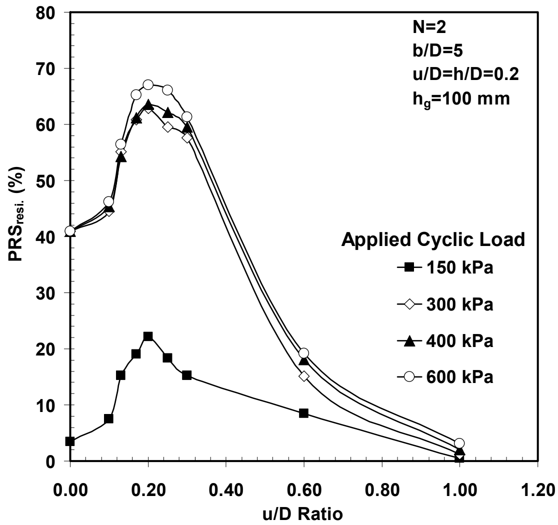

(b) $PRS_{resid.}$

Fig. 6 Variation of PRS_{total} and $PRS_{resid.}$ with u/D ratio at different amplitudes of cyclic load

in all the subsequent plate load tests, the geocell reinforcement was placed at u/D = 0.2. Yoon *et al.* (2008), in their studies using a circular plate of diameter (D) 350 mm resting on sand reinforced with multiple layers of 'Tirecell' (made from treads of waste tires), reported a similar finding for a u/D ratio (u/D = 0.2). Therefore, in the present study, use of u/D ratio of 0.2 appears defensible.

5.2 The optimum value of h/D ratio

The optimum value of the h/D ratio is the subject of Test Series 3. The tests are done for different vertical spacing of the two layers of geocell (h/D ratio). The variation of the percentage reduction in total settlement (PRS_{total}) and in residual plastic settlement ($PRS_{resid.}$) with h/B ratio at different amplitudes of cyclic load (= 150, 300, 400, 600 kPa) are shown in Fig. 7. In these tests, only one load cycle was applied. From this figure, it has been seen that with an increase in h/D ratio, regardless of the amplitude of cyclic load, the percentage reduction in the total and residual settlements (PRS_{total} and $PRS_{resid.}$) increase (i.e., the total and residual plastic settlements decrease) with increase in h/D to, approximately, 0.2. Then, with further increase in h/D ratio to 0.4 and 0.8, the values of PRS_{total} and PRS_{res} decrease. The reduction in settlements with h/D of 0.2 compared with an h/D of 0.15 could be attributed to the behaviour of the competent soil layer between the first and the second geocell layer that may be due to the effect of a soil "cushion" spreading the load over a larger area of the second geocell layer. On the other hand, at small thicknesses (e,g., h/D of 0.15 in the performed tests), it provides effective load spreading without deforming much laterally as it is confined by the geocell reinforcement above and below. However, if the reinforcing layers become too widely spaced, then the material between the geocell layers can be displaced, weakening the overall response. Generally, from Fig. 7, it is of interest to note that the percentage reduction in the total and residual settlements (PRS_{total} and PRS_{res}) are higher at higher amplitudes of cyclic load. The reason is that the reinforcing efficacy increases with increase in the penetration of loading surface as a consequence of the increase in the level of applied cyclic load.

Yoon *et al*. (2008) in their studies on circular plate with a diameter of 350 mm resting on sand reinforced with multiple layers of their 'Tirecell', reported that the effective placement of 'Tirecell' reinforcement was best at a vertical spacing of reinforcement layers of 0.2 times the plate diameter. It is of interest to note that, in spite of differences between the present study and the studies of Yoon *et al*. (2008) in the footing size, the soil properties, type of 3D reinforcement, and the geometric dimensions of the reinforcement, and the type of loading (they used the monotonic loading whereas this study also investigates unloading) the optimum values of u/D and h/D from the present study are consistent with those reported by Yoon *et al*. (2008).

Likewise, Fig. 7 shows a decrease in PRS_{total} and PRS_{res} values (corresponding to an increase in the total and residual plastic settlements), regardless of the amplitudes of cyclic load, with increasing h/D beyond the optimum value. It would be expected that, when the value of h/D reaches a thickness of 0.8-1 times the loading plate diameter, the second geocell layer would be, largely, outside of the zone of significant stress due to the surface loading, so that its influence on foundation bed behavior would become negligible and the behavior of a reinforced system with two layers of geocell would tend to that of a reinforced system supported by a single layer of geocell. The results of experimental studies conducted by Abu-Farsakh *et al*. (2008) and Chen *et al*. (2013) indicated that the vertical spacing of planar reinforcement layers needs to be less than 0.5 times of footing width to prevent the failure between reinforcement layers from occurring. Note that, the optimum vertical spacing of geocell layers beneath the loading surface, for three and four layers of geocell, might be a little different but its investigation is left for future studies.

6.3 The effect of the number of geocell layers on the settlement of loading plate

Fig. 8 illustrates the response of the pavement system in Test Series 4 (see Table 2) under the applied stress through all the cycles of loading and unloading. In this Test Series, thirty loading and unloading cycles were applied. Fifteen first cycles and fifteen second cycles were applied

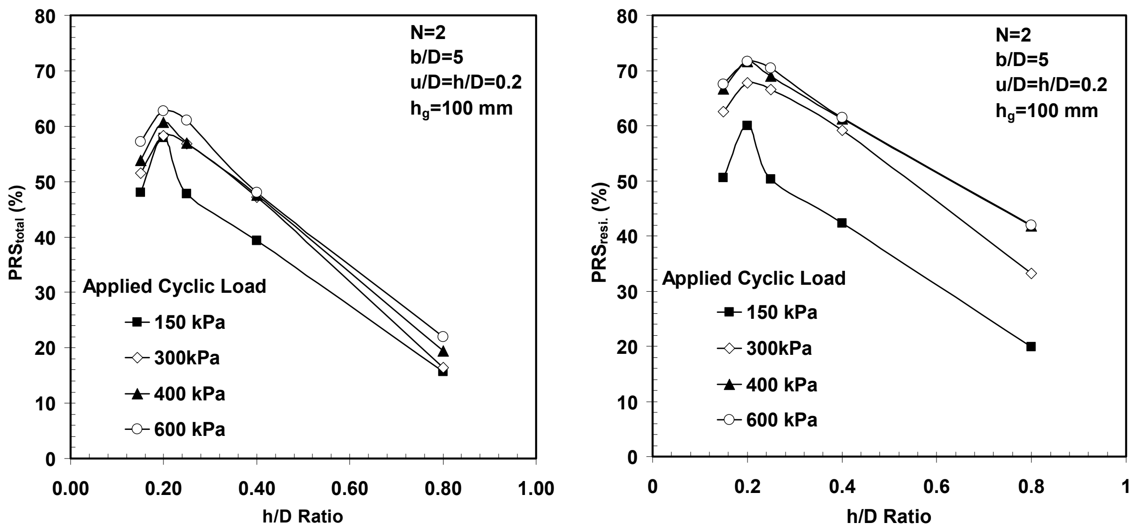

(a) PRS_{total} (b) $PRS_{resid.}$

Fig. 7 Variation of PRS_{total} and $PRS_{resid.}$ with h/D ratio at different amplitudes of cyclic load to the loading plate with amplitudes of 400 and 800 kPa, respectively. As seen in Fig. 8, for both the unreinforced and geocell reinforced bases, an initial, rapid total settlement (loading stage) and rapid residual plastic settlement (unloading stage) during the first load applications is followed by secondary settlement at the next load cycles (i.e., second, third, fourth,....., and fifteenth load cycle) that develops at a slower rate. Both the total (peak) and residual plastic settlements caused by the first cycle of applied load form a large portion of the final settlement after all cycles. Overall, in most of the tests performed on the unreinforced and the geocell reinforced foundation, the initial, rapid settlement that took place due to the first cycle of loading gave rise to between 25% and 70% of the accumulated residual plastic settlement. This ratio decreases from the unreinforced system to the geocell reinforced system. The actual proportion appears to depend on the mass of geocell and on the magnitude of the applied cyclic load.

Fig. 8 shows that for the unreinforced pavement system, the total and residual settlements tend to increase with the number of load cycles, particularly at higher levels of cyclic loads (i.e., 800 kPa). For the reinforced bases, regardless of the number of geocell layers, the rate of change of both peak and the residual settlements of the loaded surface reduces as the number of load cycles increases, so that their response has become, approximately, stable after fifteen load cycles (of both 400 and 800 kPa applied load), particularly for the reinforced bases with three and four layers of geocell. Also, it may be clearly observed that, as the number of geocell layers increases (i.e., the increase in the depth of the reinforced zone beneath the loading surface), owing to much stiffer, less peak settlement and less residual plastic settlement cause when compared with the unreinforced case, irrespective of the amplitude of applied cyclic load. For example, at 800 kPa amplitude of applied load and at load cycle number of 15, the residual settlement values are about 41.03, 33.02, 23.10, 17.43, and 15.39 mm for unreinforced bed, and geocell reinforced bed with one, two, three and four layers of geocell, respectively. Thakur *et al*. (2012) reported similar finding of the total and residual deformations with height of single geocell-reinforced bed. This behaviour might be attributable to the energy absorbance properties of geocell reinforced system that is able to exhibit a higher capacity to absorb energy than soil alone under cyclic loading and tends to decrease the stress and shocks transferred into the depth of the backfill.

The settlement reduction demonstrates that the geocell layers performed well in decreasing the soil settlement under cyclic loadings. The significant observed improvements in performance of the multi-layered geocell reinforced bed compared to that of the unreinforced bed might be attributed to the following reasons:

- The geocell reinforcement keeps the encapsulated soil from being displaced from directly beneath the applied load by confining the material by hoop action in the cell walls and behaves as a more rigid mattress, thereby increasing the shear strength of the composite system. The load redistribution that occurs within the confined zone involves a three-dimensional interaction between the infill materials and the cellular structure which spreads the applied load over an extended area, instead of directly at the point of contact, and provides a composite slab with high flexural stiffness and load support capabilities within the geocell reinforcement – consequently leading to an improvement in the overall settlement performance (Thakur *et al*. 2012, Moghaddas Tafreshi and Dawson 2010b).
- Vertical stress applied to the infill induces a horizontal active pressure at the perimeter of the cell. The infill wall interface friction transfers load into the cell structure which, in turn, mobilises resistance in surrounding cells and the geocell layers more rapidly attenuates the vertical applied stress in the soil perhaps because it is able to provide an anchorage effect on

both sides of the loaded area known as "Vertical stress dispersion effect" (Zhou and Wen 2008, Zhang *et al*. 2010). Likewise, when the depth of the plate settlement increases the deformed shape of the geocell reinforcement, consequently the geocell reinforcement can provide a further tension force due to membrane effect (Hufenus *et al*. 2006, Zhang *et al*. 2010).

In order to investigate clearly the performance of the geocell reinforcement in decreasing the total and residual settlements and increasing the resilient settlement (i.e., elastic rebound, defined

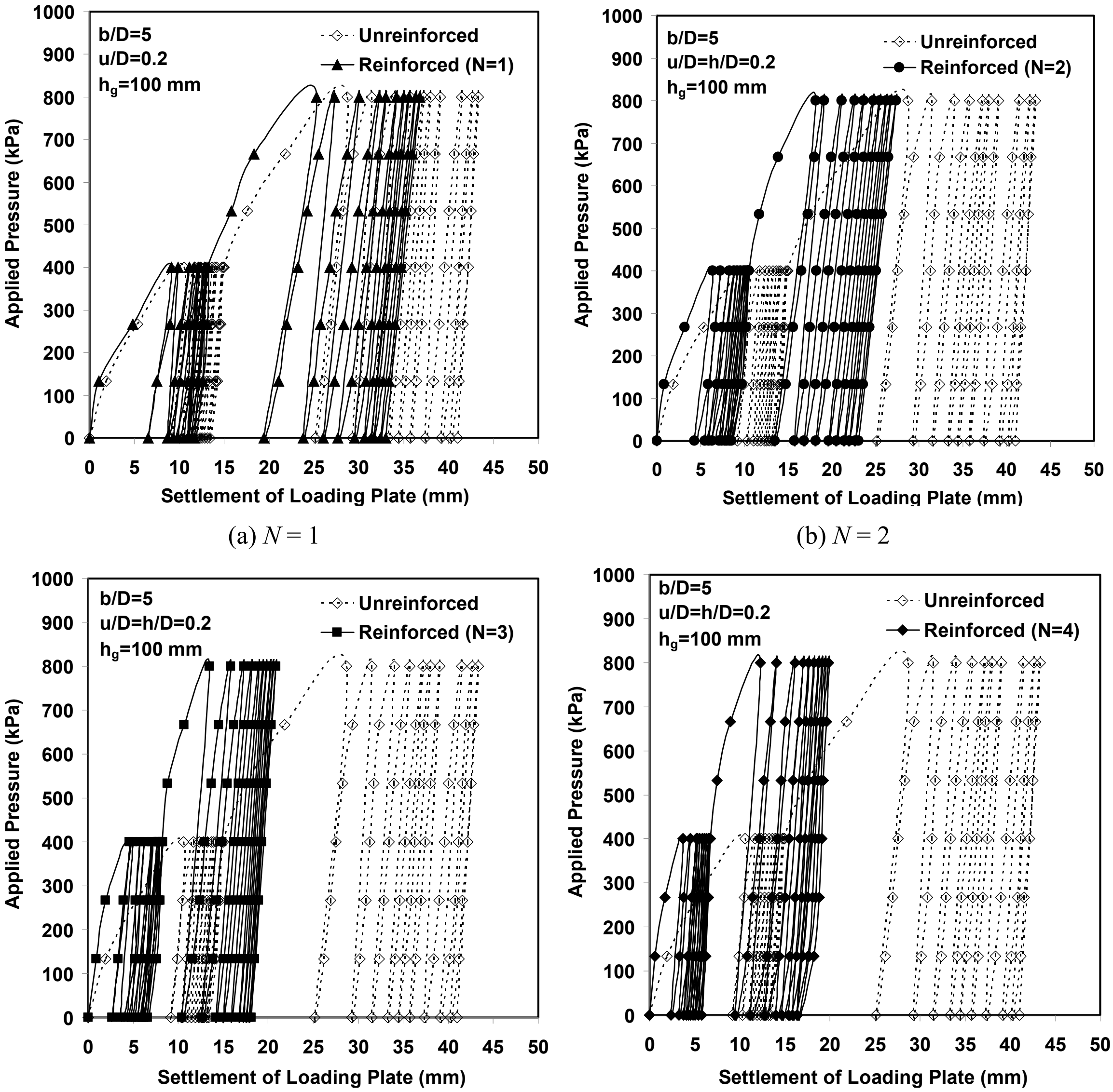

(a) $N = 1$ (b) $N = 2$

(c) $N = 3$ (d) $N = 4$

Fig. 8 Comparison between unreinforced and improved geocell-reinforced installations for different layers of geocell as the difference between the settlement under loading and under the corresponding unloading condition) of a geocell reinforced soil base, due to increase in the number of geocell layers compared to the unreinforced one, the values of percentage reduction settlement (PRS_{total} and $PRS_{resid.}$) and percentage enhancement resilient settlement ($PES_{resili.}$) are calculated at load cycle number of 5, 10, and 15, for the applied cyclic load level of 800 kPa. The variation of these three parameters, PRS_{total}, $PRS_{resid.}$, and $PES_{resil.}$ with the number of geocell layers (N) are shown in Fig. 9. Generally, from this figure, it is of interest to note that the values of PRS_{total}, $PRS_{resid.}$ and PES_{resil}. increase steadily with increase in the number of load cycles. This indicates that the reinforcing efficacy increases with increase in the number of load cycles (i.e., increase in loading surface

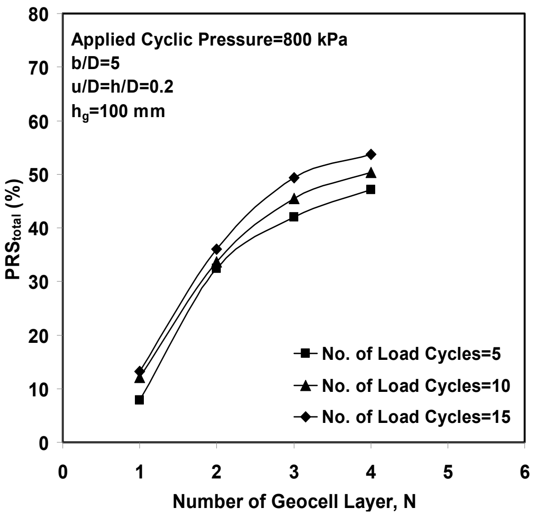

(a) PRS_{total}

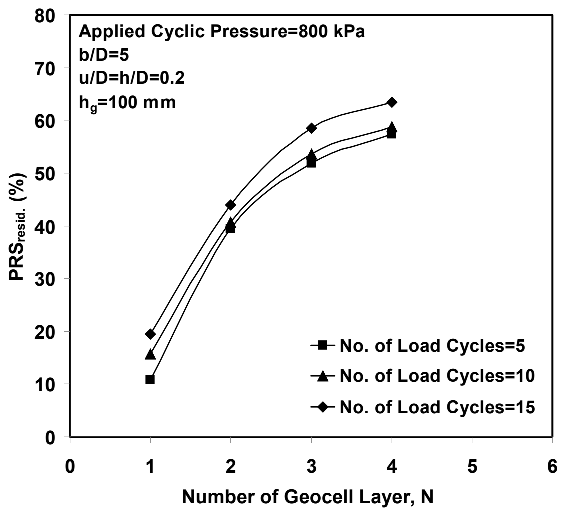

(b) $PRS_{resid.}$

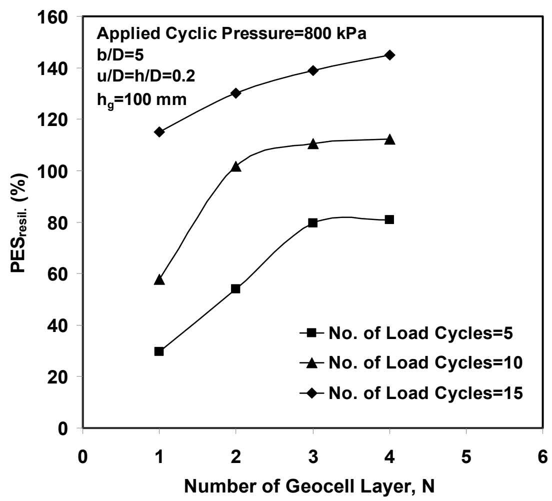

(c) PES_{resil}

Fig. 9 Variation of PRS_{total}, $PRS_{resid.}$ and PES_{resil} with the number of geocell layers at load cycle of 5, 10, and 15, for the applied cyclic load level of 800 kPa settlement), but the enhancement rate becomes insignificant with further increase in the number of load cycles (see Fig. 8).

Also, it can be seen that the values of PRS_{total}, $PRS_{resid.}$, and $PES_{resil.}$ increase steadily with increase in the number of the geocell layers. The reason is that more geocell layers considerably increases the stiffness of the reinforced bases compared to the unreinforced base. The rate of reduction in total and residual settlement and the rate of enhancement in resilient settlement of load surface can also be seen to reduce with increase in the number of geocell layers. Furthermore, one can anticipate that the improvement rates will become almost insignificant with increase in the number of geocell layers. General reason is that the zone of soil influenced by the loading extends to a depth of about 1-2 times the loading surface. Therefore, marginal performance improvement would be expected when the number of geocell layer increases to 4-5 layers. Similar results have been reported by Yoon *et al*. (2004) and Ghosh *et al*. (2005) regarding small improvements in settlement of footings and in bearing pressure of footings due to additional layers of planar reinforcement. Also, Sitharam and Siresh (2005) and Sitharam *et al*. (2007) have observed the marginal performance improvement when the height of a geocell increased to around 1.8 times of the diameter of a circular footing supported on a reinforced clay bed.

As can be seen from Fig. 9(c), at the last cycle (15th cycle) of loading and unloading of the applied load level of 800 kPa, the percentage enhancement resilient settlement ($PES_{resili.}$) are about 115%, 130%, 139%, and 145% for the reinforced bases, respectively with one, two and three layers of geocell compared to the unreinforced pavement base. Overall, the tests results reveal that the multiple geocell reinforcement improves the resilient behavior in addition to the reduction of the accumulated plastic and total settlement of the pavement foundation. This behaviour might be attributable to the restraining the soil against lateral movement with locking-up of the geocell framework, the energy absorbance properties of geocell reinforced system that is able to exhibit a higher capacity to absorb energy than soil alone under cyclic loading and tends to decrease the stress and shocks transferred into the depth of the backfill. A similar resilient response was reported for a recycled asphalt pavement base by Thakur *et al*. (2012) with height of single geocell-reinforced bed where the geocell significantly increased the proportion of deformation.

5.4 The effect of geocell layers on pressure distribution

The variation of measured pressure inside the unreinforced and the multi-layered geocell reinforced beds at the three levels of 190 mm (“SPC 1”), 350 mm (“SPC 2”), and 510 mm (“SPC 3”) beneath the center of loading plate (see Fig. 3), at 15^{th} load cycle of applied pressures of 400 and 800 kPa are given in Fig. 10. The readings of the three pressure cells show that, the pressure measured by the top soil pressure cell (“SPC 1”), may only be affected by the first layer of geocell (N = 1). On the other hand, the presence of the second or third layer of geocell has no significant effect in reducing the pressure at the depth of 190 mm (the point between first and second layers of geocell). Similarly, the pressures measured by the middle and bottom soil pressure cells (“SPC 2 and “SPC 3”) are affected, respectively, by the first two layers (N = 1, 2) and by the first three layers (N = 1, 2, 3), respectively. Thus, the stress at any depth is only affected by the construction above it and never by that below.

The results in Fig. 10 depicts that, the pressure transferred to a depth of 510 mm beneath the centre of loading plate, as measured by the bottom soil pressure cell (“SPC 3”), considerably decreases relative to the unreinforced bed, by distributing the load over a wider area as a consequence of the increase in the number of geocell layers, regardless of the level of applied load.

For example, from this figure at 15th load cycle of applied pressure of 800 kPa, the pressure values transferred to a depth of 510 mm are about 328, 190, 157, and 130 kPa for unreinforced bed, and geocell reinforced beds with one, two and three layers of geocell, respectively. This example provides clear illustration how the rate of reduction in the pressure distributed in a given depth of foundation bed reduces with increase in the number of geocell layers (N). This figure also indicates that the pressure transferred inside the foundation bed significantly reduces with depth, irrespective of the number of geocell layers and magnitude of applied load. For example, for foundation bed containing three layers of geocell (N = 3) at applied pressure of 400 kPa, the pressure measured at depths of 190, 350 and 510 mm are about 308, 95 and 39 kPa, respectively.

The effect of the amplitude of applied cyclic pressure on the pressure distributed in depth of foundation bed is clear from Fig. 10. As expected, the increase in the load value causes a direct increase in the vertical pressure for both unreinforced and geocell reinforced systems, irrespective of the number of geocell layers. Consider, for example, the vertical pressure for the geocell reinforced bed with two layers of geocell (N = 2). The pressure values at the level of 350 mm (SPC 2) beneath the center of loading plate are about 97 and 274 kPa for applied loads of 400 and 800 kPa, respectively. This example shows that the pressure transferred to this depth varies non-linearly with level of applied pressure (the measured pressure grew by a factor of 2.83 whereas the level of applied pressure only doubled). This pattern is observed irrespective of applied pressure or of soil pressure cell depth.

In order to evaluate clearly the performance of the multiple layers of geocell reinforcement in decreasing the pressure transferred through the pavement foundation compared to the unreinforced pavement one, the values of percentage reduction pressure (PRP) measured by three pressure cells (“SPC 1”, “SPC 2”, and “SPC 3”) at the first (1st) and last (15th) cycle of loadings of two levels of applied cyclic loads (= 400 and 800 kPa) are illustrated in Table 3.The data presented in this table and Fig. 10 demonstrate the performance of geocell layers, as anticipated, in reducing the pressure

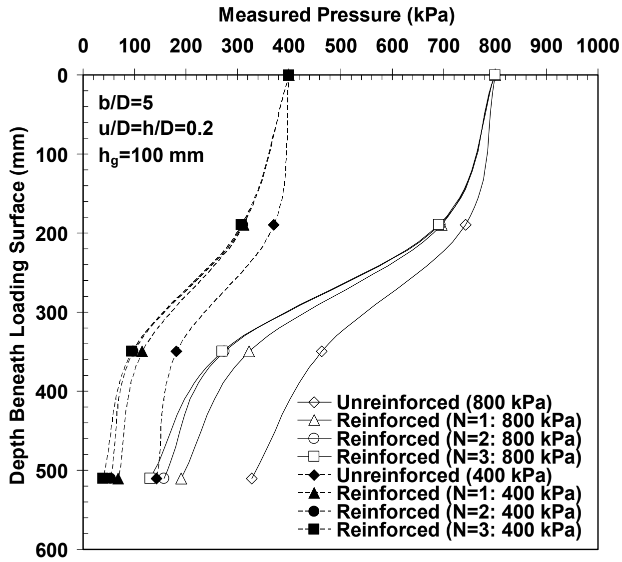

Fig. 10 Variation of measured pressure in depth of unreinforced and multi-layered gecell reinforced beds at 15^{th} load cycle of applied pressures of 400 and 800 kPa

Table 3 The percentage reduction pressure (*PRP*) measured by three pressure cells (“SPC 1”, “SPC 2”, and “SPC 3”) at the first cycle of loading (1st load cycle) and last cycle of loading (15th load cycle) of two levels of applied cyclic loads (= 400 and 800 kPa)

The values of percentage reduction pressure, PRP (%)							
Applied cyclic load (kPa)	No. of load cycle	“SPC 1”	“SPC 2”		“SPC 3”		
		$N = 1$	$N = 1$	$N = 2$	$N = 1$	$N = 2$	$N = 3$
400	1	17.5	14.3	29.1	19.7	40.8	60.6
	15	20.2	22.2	33.7	28.6	43.6	57.8
800	1	14.2	26.4	32.7	18.2	37.5	53.1
	15	17.4	30.4	40.7	21.4	43.9	56.1

transferred through the pavement foundation. For instance, the readings of “SPC 3” show that, with increase in the number of geocell layers from one layer to three, the vertical stress transferred to a depth of 510 mm beneath the center of loading surface significantly decrease, irrespective of the amplitude of cyclic load. For example, at the end of the load cycle (cycle number 15) of the applied pressure of 800 kPa, the stress measured at 510 mm depth is reduced about 21.4%, 43.9%, 56.1% for the reinforced pavement bases, respectively with one, two and three layers of geocell compared to the unreinforced pavement base. Thus as reinforcing geocell layers are added, the effective load spreading continues to improve, consequently delivering a better performance, as compared with unreinforced base. On the whole, the results show that multiple geocell layers, particularly the use of three and four layers of geocell, are able to limit the soil surface deformation and the soil pressure through the depth of the reinforced pavement foundation. Consequently an increase in road life may be anticipated under the same heavy traffic loading. The values of PRP in Table 3 also show that, a large portion of the final pressure, transferred to a depth, when the first cycle of loading is applied and then a further, smaller increase over the next cycles of loading, thereafter stabilizing to a constant value. This pattern is observed irrespective of applied pressure or of cell depth.

Generally, more stress reduction appears, when a vertical stress is transferred on the geocell layers. The layers of geocell when install at an optimum location inside the foundation bed, keep the stressed zone under the loading surface from being displaced away from the applied load by confining the material, preventing from spreading laterally, increasing the shear strength of the composite system, and thereby causing the confined composite to behave as a more rigid mattress (Koerner 2012, Zhou and Wen 2008, Zhang *et al*. 2010). This mechanism, known as “confinement effect” in literacy of soil reinforcement, allows the replaced layer to act like a large mat that spreads the applied load over an extended area, instead of directly at the point of contact, and provides a composite slab with higher flexural stiffness (Moghaddas Tafreshi and Dawson 2010a, b, Thakur *et al*. 2012), high modulus, and load support capabilities within effective zone – consequently decreasing the distributed pressure at depth in the foundation bed. Putting this another way, the geocell layers more rapidly attenuates the vertical applied stress in the soil perhaps because it is able to provide an anchorage effect on both sides of the loaded area known as “Vertical stress dispersion effect” (Zhou and Wen 2008, Zhang *et al*. 2010).

6. Conclusions

A series of cyclic circular plate load tests were conducted to investigate the effects of geocell-reinforced layers as potential pavement foundation improvement techniques. Benefits were assessed in terms of decreased settlement of pavement system (i.e., total, residual plastic and resilient settlements) and reduced pressure profile. Based on the results obtained, the following conclusions can be extracted:

(1) Both the optimum depth of the topmost layer of geocell beneath the loading surface, and the optimum vertical spacing of geocell layers should be approximately 0.2 times loading plate diameter.

(2) Installation of the geocell layers in the foundation bed, increases the resilient behavior in addition to the reduction of the accumulated plastic and total settlement of the pavement foundation due, in part, to better load spreading of the composite system and to better energy absorbance properties of geocell. Under the last cycle of loading at 800 kPa, the percentage reduction in residual settlement ($PRS_{resid.}$) are about 19%, 43%, 57%, and 63% and the percentage enhancement in resilient settlement ($PES_{resili.}$) are about 115%, 130%, 139%, and 145% for the reinforced bases, respectively with one, two and three layers of geocell compared to the unreinforced pavement base. This implies that the geocell layers act to protect the pavement from rutting due to high accumulated residual plastic settlements.

(3) The rate at which further settlement then accumulates is much slower than under the first few cycles of loading. Its occurrence appears to depend on both the mass of reinforcement and the magnitude of the cyclic load applied to the loading plate. At the low level of cyclic load (400 kPa), under fifteen load cycles applied to the loading plate, plastic shakedown (i.e., resilient response condition) occurs in all installations, irrespective of the reinforcement mass beneath the loading surface. At the high level of cyclic load (800 kPa), for the test performed on the unreinforced pavement foundation, the surface settlement is relatively large and non-stabilizing at the end of cyclic loading. For the tests performed with a high reinforcement mass (N = 3, 4), plastic shakedown occurs. When using the low reinforcement mass (N = 1, 2), the rate at which settlement accumulates under cyclic loading is significantly reduced. Shakedown was not experienced during the testing (15 cycles) but is anticipated after further cycling.

(4) Under cyclic loading, use of the geocell layers has significant effect in reducing the stress distributed down into the pavement foundation. Under the last cycle of loading at 800 kPa, the stress measured at 510 mm depth is reduced about 21.4%, 43.9%, 56.1% for the reinforced pavement bases, respectively with one, two and three layers of geocell compared to the unreinforced pavement base.

(5) With increase in the amplitude of cyclic load, the pressure transferred to a given depth varies non-linearly, irrespective of the applied pressure and the number of geocell layers. The pressure values at the level of 350 mm measured about 97 and 274 kPa for applied loads of 400 and 800 kPa, respectively. The measured pressure grew by a factor of 2.83 whereas the level of applied pressure only doubled.

(6) Since the tests results are obtained for only one type of soil, one type of geocell with one pocket size and one size of load diameter (300 mm), generalization may be needed, therefore, before these findings may be directly applied in practice. Thus, future tests with

different materials (soil and geocell) and different sizes of load diameter would be very useful and could be used to validate the present findings. Although, the results provide considerable encouragement for the use of multiple layers of geocell reinforcement for addressing localized soft pavement foundation conditions, but economic assessments of multilayered geocell reinforcement, at commercial scale would need to be performed to assure users of the applicability of the findings in every situation.

Acknowledgments

The geocell used in this study was provided by DuPont de Nemours Company in the UK (the holder of the trademark on the GroundGrid™ and Typar® products). Also, Dr. T. Amirsoleymani, the managing director of Mandro Consulting Engineers and their technicians provided the loading system, pit, some of the instrumentations and great assistance during the tests. The research is also includes results created within the projects CZ.1.07/2.3.00/30.0013 Excellence in Human Resources as a Source of Competitiveness and LO1502 Development of Regional Technological Institute. The project CZ.1.07/2.3.00/30.0013 is subsidised by the Ministry of Education, Youth and Sports from the European Social Fund and resources of the state budget of the Czech Republic. The project LO1502 is subsidised by the Ministry of Education, Youth and Sports from specific resources of the state budget for research and development.

References

Abu-Farsakh, M., Chen, Q. and Yoon, S. (2008), "Use of reinforced soil foundation (RSF) to support shallow foundation", *Louisiana Transportation Research Center* (*LTRC*), *Louisiana Department of Transportation and Development* (*LADOTD*), Report No. FHWA/LA.07/424; Baton Rouge, LA, USA, 195 p.

American Society for Testing and Materials (2009), "Standard Test Method for Repetitive Static Plate Load Tests of Soils and Flexible Pavement Components, for Use in Evaluation and Design of Airport and Highway Pavements", ASTM, D 1195-09.

American Society for Testing and Materials (2007), "Standard Test Method for Particle-Size Analysis of Soils", ASTM, D422-07.

American Society for Testing and Materials (2009), "Standard Specification for Graded Aggregate Material for Bases or Subbases for Highways or Airports", ASTM, D2940-09.

American Society for Testing and Materials (2011), "Standard Practice for Classification of Soils for Engineering Purposes (Unified Soil Classification System)", ASTM, D 2487-11.

American Society for Testing and Materials (2012), "Standard Test Methods for Laboratory Compaction Characteristics of Soil Using Modified Effort", ASTM, D 1557-12.

American Association of State Highway and Transportation Officials (AASHTO) T 221-90 (2010), Repetitive static plate load tests of soils and flexible pavement components for use in evaluation and design of airport and highway pavements.

Bathurst, R.J., Nernheim, A., Walters, D.L., Allen, T.M., Burgess, P. and Saunders, D.D. (2009), "Influence of reinforcement stiffness and compaction on the performance of four geosynthetic – reinforced soil walls", *Geosynth. Int.*, **16**(1), 43-49.

Boushehrian, A.H., Hataf, N. and Ghahramani, A. (2011), "Modeling of the cyclic behavior of shallow foundations resting on geomesh and grid-anchor reinforced sand", *Geotext. Geomembr.*, **29**(3), 242-248.

Brito, L.A.T., Dawson, A.R. and Kolisoja, P.J. (2009), "Analytical evaluation of unbound granular layers in regard to permanent deformation", *Proceedings of the 8th International on the Bearing Capacity of Roads*,

Railways, *and Airfields* (*BCR2A'09*), Champaign, IL, USA, pp. 187-196.
Chen, R.H., Huang, Y.W. and Huang, F.C. (2013), "Confinement effect of geocells on sand samples under triaxial compression", *Geotext. Geomembr*., **37**(2), 35-44.
Collin, J.G., Kinney, T.C. and Fu, X. (1996), "Full scale highway load test of flexible pavement systems with geogrid reinforced base courses", *Geosynth. Int*., **3**(4), 537-549.
Dash, S.K., Krishnaswamy, N.R. and Rajagopal, K. (2001), "Bearing capacity of strip footings supported on geocell-reinforced sand", *Geotext. Geomembr.*, **19**(4), 235-256.
Dash, S.K., Sireesh, S. and Sitharam, T.G. (2003), "Model studies on circular footing supported on geocell reinforced sand underlain by soft clay", *Geotext. Geomembr*., **21**(4), 197-219.
Dash, S.K., Rajagopal, K. and Krishnaswamy, N.R. (2007), "Behaviour of geocell reinforced sand beds under strip loading", *Can. Geotech. J*., **44**(7), 905-916.
Deb, K. and Konai, S. (2014), "Bearing capacity of geotextile-reinforced sand with varying fine fraction", *Geomech. Eng*., *Int. J*., **6**(1), 33-45.
El Sawwaf, M.A. (2007), "Behaviour of strip footing on geogrid-reinforced sand over a soft clay slope", *Geotext. Geomembr*., **25**(1), 50-60.
Ghosh, A., Ghosh, A. and Bera, A.K. (2005), "Bearing capacity of square footing on pond ash reinforced with jute-geotextile", *Geotext. Geomembr*., **23**(2), 144-173.
Hufenus, R., Rueegger, R., Banjac, R., Mayor, P., Springman, S.M. and Bronnimann, R. (2006), "Full-scale field tests on geosynthetic reinforced unpaved on soft subgrade", *Geotext. Geomembr*., **24**(1), 21-37.
Keskin, M.S. (2015), "Model studies of uplift capacity behavior of square plate anchors in geogrid-reinforced sand", *Geomech. Eng*., *Int. J*., **8**(4), 595-613.
Kim, I.T. and Tutumluer, E. (2005), "Unbound aggregate rutting models for stress rotations and effects of moving wheel loads", *Transportation Research Record*, *J. Transport. Res. Board*, **1913**, 41-49.
Koerner, R.M. (2012), *Designing with Geosynthetics*, (6th Edition), Volume 1, Xlibris Corporation, USA.
Leshchinsky, B. and Ling, H.I. (2013), "Numerical modeling of behavior of railway ballasted structure with geocell confinement", *Geotext. Geomembr*., **36**(1), 33-43.
Madhavi Latha, G. (2011), "Design of geocell reinforcement for supporting embankments on soft ground", *Geomech. Eng*., *Int. J*., **3**(2), 117-130.
Madhavi Latha, G. and Rajagopal, K. (2007), "Parametric finite element analysis of Geocell Supported Embankments", *Can. Geotech. J*., **44**(8), 917-927.
Moghaddas Tafreshi, S.N. and Dawson, A.R. (2010a), "Comparison of bearing capacity of a strip footing on sand with geocell and with planar forms of geotextile reinforcement", *Geotext. Geomembr*., **28**(1), 72-84.
Moghaddas Tafreshi, S.N. and Dawson, A.R. (2010b), "Behaviour of footings on reinforced sand subjected to repeated loading – Comparing use of 3D and planar geotextile", *Geotext. Geomembr*., **28**(5), 434-447.
Moghaddas Tafreshi, S.N. and Dawson, A.R. (2012), "A comparison of static and cyclic loading responses of foundations on geocell-reinforced sand", *Geotext. Geomembr*., **32**(5), 55-68.
Niroumand, H. and Anuar Kassim, K. (2013), "A review on uplift response of symmetrical anchor plates embedded in reinforced sand", *Geomech. Eng*., *Int. J*., **5**(3), 187-194.
Patra, C.R., Das, B.M. and Atalar, C. (2005), "Bearing capacity of embedded strip foundation on geogrid reinforced sand", *Geotext. Geomembr*., **23**(5), 454-462.
Pokharel, S.K., Han, J., Leshchinsky, D., Parsons, R.L. and Halahmi, I. (2010), "Investigation of factors influencing behavior of single geocell-reinforced bases under static loading", *Geotext. Geomembr*., **28**(6), 570-578.
Rajagopal, K., Krishanaswamy, N.R. and Latha, G.M. (1999), "Behaviour of sand confined with single and multiple geocells", *Geotext. Geomembr.*, **17**(3), 171-184.
Raymond, G.P. (2002), "Reinforced ballast behaviour subjected to repeated load", *Geotext. Geomembr*., **20**(1), 39-61.
Sitharam, T.G. and Sireesh, S. (2005), "Behavior of embedded footings supported on geogrid cell reinforced foundation beds", *Geotech. Test. J*., **28**(5), 452-463.
Sitharam, T.G., Sireesh, S. and Dash, S.K. (2007), "Performance of surface footing on geocell-reinforced soft clay beds", *Geotech. Geol. Eng*., **25**(5), 509-524.

Sireesh, S., Sailesh, P., Sitharam, T.G. and Anand, J.P. (2013), "Numerical analysis of geocell reinforced ballast overlying soft clay subgrade", *Geomech. Eng.*, *Int. J.*, **5**(3), 263-281.

Sireesh, S., Sitharam, T.G. and Dash, S.K. (2009), "Bearing capacity of circular footing on geocell–sand mattress overlying clay bed with void", *Geotext. Geomembr.*, **27**(2), 89-98.

Tandel, Y.K., Solanki, C.H. and Desai, A.K. (2014), "Field behaviour geotextile reinforced sand column", *Geomech. Eng.*, *Int. J.*, **6**(2), 195-211.

Tanyu, B.F., Aydilek, A.H., Lau, A.W., Edil, T.B. and Benson, C.H. (2013), "Laboratory evaluation of geocell-reinforced gravel subbase over poor subgrades", *Geosynth. Int.*, **20**(2), 47-61.

Tavakoli Mehrjardi, Gh., Moghaddas Tafreshi, S.N. and Dawson, A.R. (2012), "Combined use of geocell reinforcement and rubber–soil mixtures to improve performance of buried pipes", *Geotext. Geomembr.*, **34**, 116-130.

Thakur, J.K., Han, J., Pokharel, S.K. and Parsons, R.L. (2012), "Performance of geocell-reinforced recycled asphalt pavement (RAP) bases over weak subgrade under cyclic plate loading", *Geotext. Geomembr.*, **35**, 14-24.

Yang, X., Han, J., Pokharel, S.K., Manandhar, C., Parsons, R.L., Leshchinsky, D. and Halahmi, I. (2012), "Accelerated pavement testing of unpaved roads with geocell-reinforced sand bases", *Geotext. Geomembr.*, **32**, 95-103.

Yoon, Y.W., Cheon, S.H. and Kang, D.S. (2004), "Bearing capacity and settlement of tire-reinforced sands", *Geotext. Geomembr.*, **22**, 439-453.

Yoon, Y.W., Heo, S.B. and Kim, S.K. (2008), "Geotechnical performance of waste tires for soil reinforcement from chamber tests", *Geotext. Geomembr.*, **26**(1), 100-107.

Zhang, L., Zhao, M., Shi, C. and Zhao, H. (2010), "Bearing capacity of geocell reinforcement in embankment engineering", *Geotext. Geomembr.*, **28**(5), 475-482.

Zhou, H. and Wen, X. (2008), "Model studies on geogrid- or geocell-reinforced sand cushion on soft soil", *Geotext. Geomembr.*, **26**(3), 231-238.

CC

Nomenclature

b	Width of the both geocell and rubber-soil mixture layers
C_u	Coefficient of uniformity
C_c	Coefficient of curvature
D	Loading plate diameter
D_{10}	Effective grain size (mm)
D_{30}	Diameter through which 30% of the total soil mass is passing (mm)
D_{60}	Diameter through which 60% of the total soil mass is passing (mm)
G_s	Specific gravity of soil
d	Geocell pocket size
φ	Angle of shearing resistance of soil being reinforced
u	Embedded depth of the geocell
h_g	Height of geocell layers
h	Vertical spacing of the geocell layers
N	Number of geocell layers
SPC	Soil pressure cell
SPC 1	Top Soil Pressure Cell
SPC 2	Middle Soil Pressure Cell
SPC 3	Bottom Soil Pressure Cell